Inorganica Chimica Acta 374 (2011) 546–557

Contents lists available at ScienceDirect

Inorganica Chimica Acta

journal homepage: www.elsevier.com/locate/ica

Bidentate guanidine ligands with ethylene spacer in copper-dioxygen chemistry: Structural characterization of bis(μ-hydroxo) dicopper complexes

Roxana Haase [a], Tanja Beschnitt [a], Ulrich Flörke [a], Sonja Herres-Pawlis [b,]*

[a] Department Chemie, Fakultät für Naturwissenschaften, Universität Paderborn, Warburger Straße 100, 33098 Paderborn, Germany
[b] Lehrstuhl für Anorganische Chemie II, Fakultät Chemie, Technische Universität Dortmund, Otto-Hahn-Str. 6, 44227 Dortmund, Germany

ARTICLE INFO

Article history:
Available online 3 March 2011

Dedicated to Prof. W. Kaim

Keywords:
Guanidine ligands
O_2 activation
Copper
Hydroxo-bridges
UV–Vis spectroscopy
X-ray diffraction

ABSTRACT

The syntheses of the aliphatic bidentate guanidine–amine-hybrid ligands DMEGdmae (**L1**), TMGdmae (**L2**), TMGdeae (**L3**) and DPipGdmae (**L4**) as well as the reaction of their Cu(I) complexes with molecular oxygen (monitored by UV–Vis spectroscopy) are reported. The molecular structures of 10 bis(μ-hydroxo) dicopper complexes based on these ligands are described. The solid state structures of $[Cu_2(\mu\text{-OH})_2(\text{DMEGdmae})_2]X_2$ ($X^- = I^-$ (**1**), $CF_3SO_3^-$ (**2**), SbF_6^- (**3**), PF_6^- (**4**)), $[Cu_2(\mu\text{-OH})_2(\text{TMGdmae})_2]X_2$ ($X^- = I^-$ (**5**), $CF_3SO_3^-$ (**6**)), $[Cu_2(\mu\text{-OH})_2(\text{TMGdeae})_2]Cu_2I_4$ (**7**) and $[Cu_2(\mu\text{-OH})_2(\text{DPipGdmae})_2]X_2$ ($X^- = CF_3SO_3^-$ (**8**), SbF_6^- (**9**), PF_6^- (**10**)) show a square-planar distorted coordination of the copper(II) ion. The bis(μ-hydroxo) dicopper complex **1** exhibits a Cu···Cu distance of 2.860(1) Å, which is one of the smallest observed for hydroxo-bridged copper compounds so far. The influence of the anion on the structure of the bis(μ-hydroxo) dicopper(II) unit is analyzed for the reported complexes and a literature overview with emphasis on the structural characteristics of the Cu_2O_2 moiety of bis(μ-hydroxo) dicopper(II) and bis(μ-oxo) dicopper(III) is given.

1. Introduction

The activation and transfer of molecular oxygen by copper centers plays an important role in biological and technical oxidation processes. Functional model complexes for the active site of dioxygen binding and activating copper enzymes like tyrosinase have been studied for more than 30 years and are primarily aimed at the development of technically recoverable oxidation catalysts. For such model complexes the ligand design is of vital importance. On one hand the ligands should stabilize the reactive Cu_2O_2 species, which are formed by the reaction of the copper(I) complex with molecular oxygen. On the other hand they may not shield the reaction center too much for external substrates, so that the efficiency of oxygen transfer is not reduced [1–27].

Recently, we reported that guanidine–amine-hybrid ligands proved to be particularly suited for the chemical modeling of tyrosinase [25,27]. Besides the excellent donor properties of the guanidine function, the main reason for this reactivity was related to the open coordination space that is created by the smaller amine function and facilitates the entry of a substrate to the Cu_2O_2 center. The superior biomimetic hydroxylation activity of the bis(μ-oxo)dicopper guanidine–amine-hybrid complex $[Cu_2(\text{TMGdmap})_2(\mu\text{-O})_2][CF_3SO_3]_2$ (Fig. 1a) compared to the parent bisguanidine (Fig. 1b) and bisamine systems (Fig. 1c) has shown that the improved accessibility of the active Cu_2O_2 center is associated with an increase of the hydroxylation reactivity. For this reason, additional guanidine–amine-hybrid ligands were developed and the influence of the substituents on the formation and stability of the Cu_2O_2 species was examined. With regard to the ligand TMGdmap which possesses a propylene spacer, the new hybrid ligands comprise an ethylene spacer between the two N donor functions. Furthermore, the characterization of the thermal decomposition products of the Cu_2O_2 complexes provides additional information on the complexation properties of the ligands.

Herein, we report the synthesis and characterization of the guanidine–amine-hybrid ligands N^1-(1,3-dimethylimidazolidin-2-yliden)-N^2,N^2-dimethylethan-1,2-diamine (DMEGdmae, **L1**), 2-(2-(dimethylamino)ethyl)-1,1,3,3-tetramethylguanidine (TMGdmae, **L2**), [28,29][1] 2-(2-(diethylamino)ethyl)-1,1,3,3-tetramethylguanidine (TMGdeae, **L3**) and N^1-(dipiperidin-1-ylmethylen)-N^2,N^2-dimethylethan-1,2-diamine (DPipGdmae, **L4**) (Scheme 1). After synthesis of their copper(I) complexes, their reaction with O_2 was monitored by means of UV–Vis spectroscopy. Only in case of **L2**, a bis(μ-oxo) dicopper complex could be detected. With ligands **L1**, **L2** and **L4**, several examples of bis(μ-hydroxo) dicopper

---

[1] TMGdmae has been identified by Raczyńska et al. using mass spectrometry in the gas phase, but not isolated and was therefore not yet suitable for use in complex chemistry.

* Corresponding author.
E-mail address: sonja.herres-pawlis@tu-dortmund.de (S. Herres-Pawlis).

0020-1693/$ - see front matter © 2011 Elsevier B.V. All rights reserved.
doi:10.1016/j.ica.2011.02.061

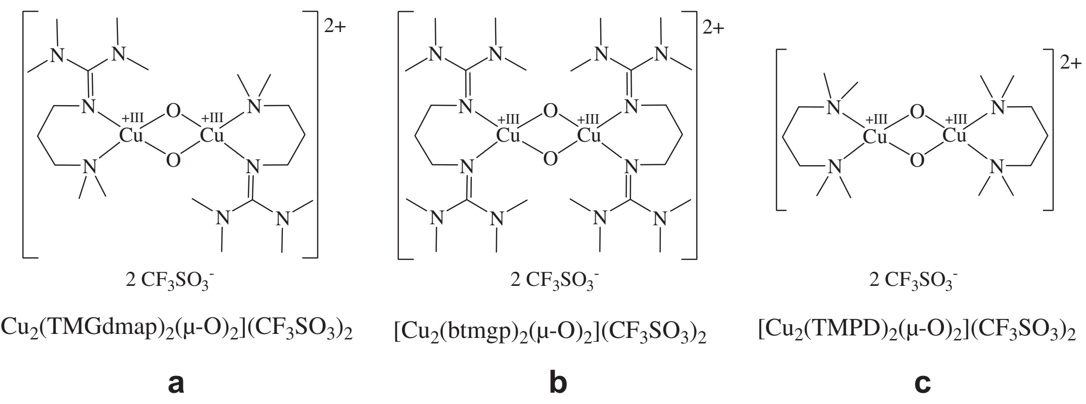

Fig. 1. Bis(μ-oxo) dicopper complex of (a) the guanidine–amine-hybrid ligand TMGdmap, (b) the bisguanidine ligand btmgp and (c) the bisamine ligand TMPD.

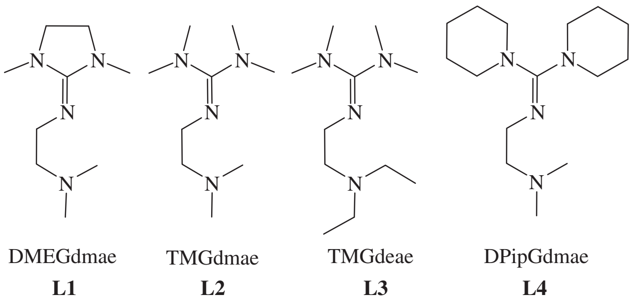

Scheme 1. Synthesized guanidine–amine-hybrid ligands.

complexes could be isolated and structurally characterized.

2. Experimental

2.1. Synthesis and characterization of guanidine–amine-hybrid ligands

To a solution of a primary amine (40 mmol) and triethylamine (40 mmol) in 40 mL of dry MeCN a solution of the chloroformamidinium chloride (40 mmol) in 40 mL of dry MeCN was added dropwise under vigorous stirring and ice cooling. After 3 h at reflux, 10 mL of aqueous NaOH (40 mmol, 1.6 g) were added, and the volatile organics were removed under vacuum. For the deprotonation of the formed guanidine hydrochloride 10 mL of 50% KOH solution were added to the residue. Finally the free base was extracted into MeCN (3 × 30 mL), dried under Na_2SO_4 and after filtration the solvent was evaporated under reduced pressure.

*2.1.1. N^1-(1,3-Dimethylimidazolidin-2-yliden)-N^2,N^2-dimethylethan-1,2-diamine (DMEGdmae, **L1**)*

Used amine: 2-(Dimethylamino)ethylamine, used Vilsmeier salt: *N,N,N′,N′*-Dimethylethylenechloroformamidinium chloride, product: yellow oil, yield: 92% (6.78 g, 36.8 mmol).^{1}H NMR (500 MHz, $CDCl_3$, 25 °C, δ [ppm]): 2.09 (s, 6H, CH_3), 2.27–2.30 (m, 2H, CH_2), 2.60 (s, 6H, CH_3), 2.96 (s, 4H, CH_2), 3.30–3.33 (m, 2H, CH_2). ^{13}C NMR (125 MHz, $CDCl_3$, 25 °C, δ [ppm]): 36.1 (CH_3), 46.0 (CH_3), 46.2 (CH_2,), 49.2 (CH_2), 62.8 (CH_2), 157.2 (C_{gua}). EI-MS (*m/z*, (%)): 184.2 (10) [M^+], 126 (100) [M^+–$H_2CN(CH_3)_2$], 114 (5), 98 (5), 85 (12), 70 (10), 58 (21) [$H_2CN(CH_3)_2{}^+$], 56 (22), 42 (18). IR (film between NaCl plates, $\tilde{\nu}$ [cm^{-1}]): 2939 *m*, 2817 *m*, 2765 *m*, 1666 *vs* (ν(C=N)), 1558 *vw*, 1541 *vw*, 1481 *m*, 1460 *m*, 1439 *m*, 1412 *w*, 1383 *m*, 1317 *vw*, 1265 *m*, 1198 *w*, 1180 *w*, 1151 *vw*, 1119 *vw*, 1097 *w*, 1086 *w*, 1068 *w*, 1041 *w*, 1018 *m*, 987 *w*, 957 *m*, 928 *vw*, 914 *vw*.

*2.1.2. 2-(2-(Dimethylamino)ethyl)-1,1,3,3-tetramethylguanidine (TMGdmae, **L2**)*

Used amine: 2-(Dimethylamino)ethylamine, used Vilsmeier salt: *N,N,N′,N′*-Tetramethylchloroformamidinium chloride, product: yellow oil, yield: 90% (6.70 g, 36.0 mmol).^{1}H NMR (500 MHz, $CDCl_3$, 25 °C, δ [ppm]): 2.22 (s, 6H, CH_3), 2.40–2.43 (m, 2H, CH_2), 2.61 (s, 6H, CH_3), 2.70 (s, 6H, CH_3), 3.20–3.23 (m, 2H, CH_2).^{13}C NMR (125 MHz, $CDCl_3$, 25 °C, δ [ppm]): 38.8 (CH_3), 39.6 (CH_3), 46.0 (CH_3) , 48.3 (CH_2), 62.3 (CH_2), 160.5 (C_{Gua}). EI-MS (*m/z*, (%)): 186.2 (10) [M^+], 142 (18) [M^+–$N(CH_3)_2$], 128 (80) [M^+–$H_2CN(CH_3)_2$], 112 (3), 97 (4), 86 (16), 85 (100), 72 (28) [M^+–N=C($N(CH_3)_2)_2$], 58 (48) [$H_2CN(CH_3)_2{}^+$], 42(20). IR (film between NaCl plates, $\tilde{\nu}$ [cm^{-1}]): 2937 *m*, 2883 *m*, 2813 *m*, 2789 *m*, 2765 *m*, 1622 *vs* (ν(C=N)), 1496 *m*, 1454 *m*, 1404 *vw*, 1365 *s*, 1306 *vw*, 1236 *w*, 1132 *m*.

*2.1.3. 2-(2-(Diethylamino)ethyl)-1,1,3,3-tetramethylguanidine (TMGdeae, **L3**)*

Used amine: 2-(Diethylamino)ethylamine, used Vilsmeier salt: *N,N,N′,N′*-Tetramethylchloroformamidinium chloride, product: yellow oil, yield: 88% (7.58 g, 35.4 mmol).^{1}H NMR (500 MHz, $CDCl_3$, 25 °C, δ [ppm]): 1.01 (t, 6H, CH_3, ^3J = 7.18 Hz), 2.52–2.58 (m, 6H, CH_2), 2.64 (s, 6H, CH_3), 2.72 (s, 6H, CH_3), 3.20–3.23 (m, 2H, CH_2). ^{13}C NMR (500 MHz, $CDCl_3$, 25 °C, δ [ppm]): 11.8 (CH_3), 38.8 (CH_3), 39.6 (CH_3), 47.6 (CH_2), 48.2 (CH_2), 55.8 (CH_2), 160.5 (C_{gua}). EI-MS (*m/z* (%)): 214.2 (33) [M^+], 185 (14) [M^+–CH_2CH_3], 143 (26), 128 (90) [M^+–$H_2CN(CH_2CH_3)_2$], 126 (63), 100 (35) [M^+–N=C($N(CH_3)_2)_2$], 86 (85) [$H_2CN(CH_2CH_3)_2{}^+$], 85 (100), 72 (30)[$N(CH_2CH_3)_2{}^+$], 58 (31), 56 (21), 44 (24)[$N(CH_3)_2{}^+$], 42 (20). IR (film between NaCl plates, $\tilde{\nu}$ [cm^{-1}]): 2968 *s*, 2931 *s*, 2871 *s*, 2839 *s*, 2798 *s*, 1622 *vs* (ν(C=N)), 1558 *vw*, 1539 *vw*, 1496 *m*, 1452 *m*, 1404 *w*, 1365 *s*, 1292 *w*, 1236 *w*, 1203 *w*, 1174 *vw*, 1134 *m*, 1065 *m*, 993 *w*, 914 *w*.

*2.1.4. N^1-(Dipiperidin-1-ylmethylen)-N^2,N^2-dimethylethan-1,2-diamine (DPipGdmae, **L4**)*

Used amine: 2-(Dimethylamino)ethylamine, used Vilsmeier salt: Dipiperidin-1-yl-chloroformamidinium chloride, product: yellow oil, yield: 88% (9.36 g, 35.2 mmol).^{1}H NMR (500 MHz, $CDCl_3$, 25 °C, δ [ppm]):1.41–1.43 (m, 12H, CH_2), 2.13 (s, 6H, CH_3), 2.33–2.36 (m, 2H, CH_2), 2.88–2.91 (m, 4H, CH_2), 2.94–2.96 (m, 4H, CH_2), 3.13–3.16 (m, 2H, CH_2). ^{13}C NMR (125 MHz, $CDCl_3$, 25 °C, δ [ppm]): 24.7 (CH_2), 25.8 (CH_2), 45.8 (CH_3), 47.2 (CH_2), 48.9 (CH_2), 61.6 (CH_2), 160.0 (C_{Gua}). EI-MS (*m/z*, (%)): 266.2 (12) [M^+], 208 (52) [M^+–$H_2CN(CH_3)_2$], 196 (75), 139 (12), 126 (69), 125 (97), 113 (48), 112 (93), 100 (58), 86 (38), 85 (84), 84 (100) [$H_{10}C_5N^+$], 83 (59), 72 (19) [$H_4C_2N(CH_3)_2{}^+$], 70 (37), 69 (92), 56 (59), 42 (37), 41(74). IR (film between NaCl plates, $\tilde{\nu}$ [cm^{-1}]):

2969 *w*, 2931 *vs*, 2850 *s*, 2815 *m*, 2765 *w*, 1646 m, 1616 *vs* (ν(C=N)), 1558 *vw*, 1521 *vw*, 1506 *vw*, 1450 *w*, 1440 *m*, 1403 *m*, 1371 *m*, 1347 *w*, 1324 *vw*, 1249 *vs*, 1213 *s*, 1182 *w*, 1155 *w*, 1130 *s*.

2.2. Synthesis and characterization of bis(μ-hydroxo) dicopper guanidine–amine-hybrid complexes

At first the copper(I) complexes were synthesised in situ by reaction of 0.1 mmol of ligand with 0.1 mmol of the corresponding copper(I) salt in 5 mL of MeCN at room temperature in a glove-box under nitrogen [25]. For the preparation of the bis(μ-hydroxo) dicopper complexes, 0.5 mL of this copper(I) solution was injected into 10 mL of oxygenated THF or MeCN at 298 K. By vapor diffusion of diethyl ether into this solution suitable crystals for X-ray diffraction can be obtained after a few weeks. Solvents were purified according to the literature procedures and also kept under nitrogen.

*2.2.1. Complex salt **1**, $[Cu_2(\mu\text{-}OH)_2(DMEGdmae)_2]I_2$*

Violet crystals, yield: 37%. EI-MS (*m*/*z*, (%)): 184 (9) [DMEGdmae$^+$], 127 (48), 126 (100) [DMEGdmae$^+$–$H_2CN(CH_3)_2$], 114 (6), 85 (10), 70 (14), 58 (32) [$H_2CN(CH_3)_2^+$], 56 (43), 42 (31). IR (KBr, $\tilde{\nu}$ [cm^{-1}]): 3404 *m* (ν(OH)), 2958 *w*, 2924 *w*, 2862 *w*, 1604 *vs* (ν(C=N)), 1504 *m*, 1473 *w*, 1429 *w*, 1400 *w*, 1581 *vw*, 1344 *vw*, 1294 *m*, 1275 *w*, 1236 *vw*, 1201 *vw*, 1165 *vw*, 1124 *vw*, 1092 *vw*, 1078 *vw*, 1036 *vw*, 1022 *w*, 980 *vw*, 953 *vw*, 916 *vw*, 883 *vw*, 849 *vw*, 808 *vw*, 771 *w*, 733 *vw*, 700 *vw*, 669 *vw*, 650 *vw*, 606 *vw*, 567 *vw*.

*2.2.2. Complex salt **2**, $[Cu_2(\mu\text{-}OH)_2(DMEGdmae)_2][(CF_3SO_3)_2]$*

Violet crystals, yield: 60%. EI-MS (*m*/*z*, (%)): 184 (6) [DMEGdmae$^+$], 168 (13), 127 (30), 126 (100) [DMEGdmae$^+$–$H_2CN(CH_3)_2$], 112 (85) [DMEGdmae$^+$–$H_4C_2N(CH_3)_2$], 100 (75), 83 (16), 71 (39), 70 (31), 58 (98) [$H_2CN(CH_3)_2^+$], 56 (66), 44 (71) [$N(CH_3)_2^+$], 42 (78). IR (KBr, $\tilde{\nu}$ [cm^{-1}]): 3433 *m* (ν(OH)), 2963 *vw*, 2924 *vw*, 2886 *vw*, 2854 *vw*, 1610 *s* (ν(C=N)), 1544 *vw*, 1509 *vw*, 1491 *vw*, 1468 *w*, 1449 *vw*, 1430 *vw*, 1399 *vw*, 1383 *vw*, 1350 *vw*, 1274 *s*, 1261 *s*, 1224 *vw*, 1187 *vw*, 1149 *m*, 1098 *w*, 1075 *vw*, 1035 *m*, 955 *vw*, 921 *vw*, 806 *w*, 782 *vw*, 753 *vw*, 724 *vw*, 708 *w*, 640 *m*, 572 *vw*, 517 *w*.

*2.2.3. Complex salt **3**, $[Cu_2(\mu\text{-}OH)_2(DMEGdmae)_2][(SbF_6)_2]$*

Violet crystals, yield: 73%. EI-MS (*m*/*z*, (%)): 184 (5) [DMEGdmae$^+$], 127 (25), 126 (100) [DMEGdmae$^+$–$H_2CN(CH_3)_2$], 114 (29), 100 (9), 85 (8), 82 (8), 72 (10), 70 (11), 58 (90) [$H_2CN(CH_3)_2^+$], 56 (37), 44 (25) [$N(CH_3)_2^+$], 42 (52). IR (KBr, $\tilde{\nu}$ [cm^{-1}]): 3618 *m* (ν (OH)), 3012 *w*, 2987 *w*, 2947 *m*, 2902 *m*, 2875 *w*, 2846 *w*, 2815 *vw*, 2802 *vw*, 1612 *s* (ν(C=N)), 1508 *m*, 1487 *m*, 1460 *s*, 1425 *s*, 1398 *s*, 1383 *w*, 1342 *m*, 1292 *vs*, 1255 *m*, 1236 *m*, 1200 *w*, 1186 *vw*, 1138 *vw*, 1105 *w*, 1084 *m*, 1043 *w*, 1032 *m*, 1016 *m*, 978 *w*, 958 *s*, 918 *m*, 881 *vw*, 856 *w*, 814 *w*, 769 *m*, 731 *m*, 717 *vw*, 660 *vs*, 642 *vs*, 619 *m*, 607 *m*, 569 *vw*, 505 *m*.

*2.2.4. Complex salt **4**, $[Cu_2(\mu\text{-}OH)_2(DMEGdmae)_2][(PF_6)_2]$*

Black crystals, yield: 67%. EI-MS (*m*/*z*, (%)): 184 (15) [DMEGdmae$^+$], 140 (10) [DMEGdmae$^+$–$N(CH_3)_2$], 127 (79), 126 (100) [DMEGdmae$^+$–$H_2CN(CH_3)_2$], 113 (54), 112 (53) [DMEGdmae$^+$–$H_4C_2N(CH_3)_2$], 107 (50), 100 (12), 98 (15), 85 (20), 82 (27), 70 (54), 58 (93) [$H_2CN(CH_3)_2^+$], 56 (87), 44 (60) [$N(CH_3)_2^+$], 42 (90). IR (KBr, $\tilde{\nu}$ [cm^{-1}]): 3609 *m* (ν(OH)), 3008 *w*, 2985 *w*, 2939 *w*, 2903 *w*, 2884 *m*, 2846 *w*, 2816 *vw*, 2800 *vw*, 1615 *vs* (ν(C=N)), 1508 *m*, 1460 *m*, 1427 *m*, 1399 *m*, 1382 *w*, 1341 *w*, 1292 *m*, 1255 *w*, 1236 *w*, 1198 *vw*, 1184 *vw*, 1137 *vw*, 1106 *vw*, 1084 *w*, 1043 *vw*, 1031 *w*, 1017 *w*, 978 *vw*, 960 *m*, 918 *w*, 840 *vs*, 770 *w*, 732 *w*, 648 *vw*, 607 *vw*, 558 *s*, 504 *m*.

*2.2.5. The complex salt **5**, $[Cu_2(\mu\text{-}OH)_2(TMGdmae)_2]I_2$*

Violet crystals, yield: 44%. EI-MS (*m*/*z*, (%)): 186 (57) [TMGdmae$^+$], 142 (65) [TMGdmae$^+$–$N(CH_3)_2$], 129 (64), 128 (93) [TMGdmae$^+$–$H_2CN(CH_3)_2$], 112 (12), 100 (15), 97 (29), 86 (74), 85 (100), 72 (98) [$H_4C_2N(CH_3)_2^+$], 69 (72), 58 (91) [$H_2CN(CH_3)_2^+$], 56 (59), 44 (67) [$N(CH_3)_2^+$], 42(99). IR (KBr, $\tilde{\nu}$ [cm^{-1}]): 3365 *m* (ν (OH)), 3001 *vw*, 2985 *vw*, 2935 *w*, 2891 *w*, 2810 *vw*, 1579 *vs* (ν(C=N)), 1533 *s* (ν(C=N)), 1471 *w*, 1458 *w*, 1441 *w*, 1427 *w*, 1392 *s*, 1346 *vw*, 1331 *vw*, 1281 *vw*, 1254 *vw*, 1238 *vw*, 1159 *w*, 1138 *vw*, 1111 *vw*, 1084 *vw*, 1068 *vw*, 1043 *vw*, 1022 *vw*, 958 *vw*, 922 *vw*, 897 *vw*, 808 *vw*, 768 *vw*, 735 *vw*, 708 *vw*, 677 *vw*, 650 *vw*, 617 *vw*, 592 *vw*, 573 *vw*, 503 *vw*.

*2.2.6. Complex salt **6**, $[Cu_2(\mu\text{-}OH)_2(TMGdmae)_2][(CF_3SO_3)_2]$*

Black crystals, yield: 55%. EI-MS (*m*/*z*, (%)): 186 (22) [TMGdmae$^+$], 142 (21) [TMGdmae$^+$–$N(CH_3)_2$], 139 (18), 128 (90) [TMGdmae$^+$–$H_2CN(CH_3)_2$], 126 (42), 116 (17), 115 (39), 97 (12), 86 (43), 85 (100), 72 (94) [$H_4C_2N(CH_3)_2^+$], 71 (80), 69 (55), 58 (94) [$H_2CN(CH_3)_2^+$], 44 (77) [$N(CH_3)_2^+$], 42 (81). IR (KBr, $\tilde{\nu}$ [cm^{-1}]): 3492 *s* (ν(OH)), 3010 *w*, 2936 *m*, 2884 *m*, 2813 *vw*, 2787 *vw*, 1580 *vs* (ν(C=N)), 1538 *vs* (ν(C=N)), 1467 *s*, 1453 *s*, 1430 *s*, 1400 *vs*, 1334 *m*, 1275 *vs*, 1256 *vs*, 1220 *vs*, 1157 *vs*, 1111 *w*, 1080 *m*, 1070 *w*, 1026 *vs*, 958 *m*, 923 *m*, 897 *m*, 809 *m*, 768 *m*, 755 *w*, 729 *vw*, 706 *vw*, 622 *vs*, 593 *w*, 571 *m*, 516 *vs*.

*2.2.7. Complex salt **7**, $[Cu_2(\mu\text{-}OH)_2(TMGdeae)_2]Cu_2I_4$*

Black crystals, yield: 70%. EI-MS (*m*/*z* (%)): 214 (11) [TMGdeae$^+$], 143 (12), 128 (90) [M$^+$–$H_2CN(CH_2CH_3)_2$], 126 (14), 100 (22) [M$^+$–N=$C(N(CH_3)_2)_2$], 85 (100), 72 (63) [$N(CH_2CH_3)_2^+$], 58 (28), 56 (18), 44 (34) [$N(CH_3)_2^+$], 42 (28). IR (KBr, $\tilde{\nu}$ [cm^{-1}]): 3433 *w* (ν(OH)), 3002 *vw*, 2975 *m*, 2939 *m*, 2879 *m*, 2805 *vw*, 1572 *vs* (ν(C=N)), 1532 *vs* (ν(C=N)), 1459 *s*, 1440 *s*, 1427 *s*, 1361 *m*, 1347 *m*, 1332 *m*, 1261 *m*, 1232 *m*, 1185 *vw*, 1165 *m*, 1147 *m*, 1115 *w*, 1080 *m*, 1063 *m*, 1052 *m*, 1003 *m*, 933 *vw*, 897 *w*, 838 *vw*, 792 *m*, 744 *vw*, 726 *vw*, 591 *vw*, 566 *vw*, 492 *m*.

*2.2.8. Complex salt **8**, $[Cu_2(\mu\text{-}OH)_2(DPipGdmae)_2][(CF_3SO_3)_2]$*

Violet crystals, yield: 44%. EI-MS (*m*/*z*, (%)): 266 (4) [DPipGdmae$^+$], 208 (45) [DPipGdmae$^+$–$H_2CN(CH_3)_2$], 196 (18), 125 (100), 112 (19), 98 (13), 84 (96) [$H_{10}C_5N^+$], 72 (15) [$H_4C_2N(CH_3)_2^+$], 69 (34), 58 (50) [$H_2CN(CH_3)_2^+$], 44 (24) [$N(CH_3)_2^+$], 42 (38). IR (KBr, $\tilde{\nu}$ [cm^{-1}]): 3365 *m* (ν(OH)), 2993 *w*, 2935 *m*, 2854 *m*, 1554 *vs* (ν(C=N)), 1500 *s*, 1444 *m*, 1408 *vw*, 1373 *w*, 1356 *vw*, 1336 *w*, 1284 *vs*, 1252 *vs*, 1223 *m*, 1190 *vw*, 1145 *s*, 1109 *w*, 1068 *vw*, 1028 *vs*, 987 *vw*, 955 *w*, 922 *w*, 854 *w*, 795 *vw*, 750 *w*, 636 *s*, 570 *w*, 514 *m*.

*2.2.9. Complex salt **9**, $[Cu_2(\mu\text{-}OH)_2(DPipGdmae)_2][(SbF_6)_2]$*

Violet crystals, yield: 35%. EI-MS (*m*/*z*, (%)): 266 (3) [DPipGdmae$^+$], 208 (30) [DPipGdmae$^+$–$H_2CN(CH_3)_2$], 195 (7), 194 (7), 180 (17), 178 (24), 167 (34), 160 (45), 159 (51), 138 (41), 125 (100), 112 (22), 98 (18), 84 (70) [$H_{10}C_5N^+$], 69 (15), 58 (14) [$H_2CN(CH_3)_2^+$], 56 (20), 42 (18). IR (KBr, $\tilde{\nu}$ [cm^{-1}]): 3604 *w* (ν(OH)), 3010 *vw*, 2889 *vw*, 2943 *m*, 2856 *m*, 1560 *vs* (ν(C=N)), 1496 *s*, 1468 *m*, 1444 *s*, 1410 *vw*, 1373 *m*, 1356 *w*, 1336 *m*, 1273 *m*, 1252 *s*, 1227 *w*, 1190 *vw*, 1161 *vw*, 1136 *m*, 1109 *w*, 1036 *w*, 1016 *w*, 987 *vw*, 955 *vw*, 924 *vw*, 914 *vw*, 891 *vw*, 872 *w*, 854 *m*, 839 *vw*, 795 *w*, 748 *w*, 661 *vs*, 640 *s*, 569 *vw*, 515 *w*, 507 *w*.

*2.2.10. Complex salt **10**, $[Cu_2(\mu\text{-}OH)_2(DPipGdmae)_2][(PF_6)_2]$*

Violet crystals, yield: 45%. EI-MS (*m*/*z*, (%)): 266 (4) [DPipGdmae$^+$], 208 (44) [DPipGdmae$^+$–$H_2CN(CH_3)_2$], 196 (17), 125 (100), 112 (19), 107 (23), 98 (19), 84 (99) [$H_{10}C_5N^+$], 72 (17) [$H_4C_2N(CH_3)_2^+$], 69 (35), 58 (82) [$H_2CN(CH_3)_2^+$], 42 (47), 41 (47). IR (KBr, $\tilde{\nu}$ [cm^{-1}]): 3593 *m* (ν(OH)), 2947 *m*, 2927 *m*, 2860 *w*, 1552 *s* (ν(C=N)), 1489 *m*, 1441 *m*, 1375 *vw*, 1356 *vw*, 1334 *w*, 1282 *w*, 1271 *w*, 1252 *m*, 1225 *vw*, 1190 *vw*, 1159 *vw*, 1130 *vw*, 1105 *vw*, 1072 *vw*, 1038 *vw*, 1014 *w*, 953 *w*, 843 *vs*, 791 *w*, 752 *vw*, 739 *vw*, 717 *vw*, 636 *vw*, 602 *vw*, 557 *m*, 519 *vw*.

2.3. Measurements

Spectra were recorded with the following spectrometers: NMR: BrukerAvance 500. The signals were calibrated to the residual signals of the deuterated solvent ($\delta_H(CDCl_3)$ = 7.26 ppm). IR: Nicolet P510. MS (EI, 70 eV): Finnigan MAT 8200. UV–Vis: Perkin-Elmer Lambda 45 with a low-temperature fiber-optic interface (Hellma; 1 mm) and a custom-designed Schlenk cell with compression fittings.

2.4. X-ray structure analyses

The X-ray intensities of the bis(μ-hydroxo) dicopper complexes were collected at 120 K on a Bruker-AXS Smart [30] APEX CCD-diffractometer with graphite monochromated Mo Kα radiation (λ = 0.71073 Å). The structures were solved by direct and conventional Fourier methods and refined on F^2 by full-matrix least-squares techniques using SHELXTL [31].

Selected crystallographic data of the compounds are summarized in Table 1.

2.5. UV–Vis spectroscopy of the oxygenation of Cu(I) precursor complexes

Solutions for optical investigations were generally prepared in situ by initially mixing equimolar amounts of a Cu(I) salt $[Cu(MeCN)_4](CF_3SO_3)_2$, $[Cu(MeCN)_4](SbF_6)_2$ with the guanidine–amine-hybrid ligands **L1**–**L4**. Oxygenation proceeded by rapid injection of a concentrated Cu(I) complex solution (2 mM) into preoxygenated THF at 195 K.

3. Results and discussion

3.1. Synthesis of the guanidine–amine-hybrid ligands

The preparation of guanidine–amine-hybrid ligands was carried out according to the approved synthesis protocol of Kantlehner et al. [32] by condensation of the chloroformamidinium chloride (Vilsmeier salts) with primary aliphatic amines (Fig. 2). The required Vilsmeier salts are accessible in good yields from the appropriately substituted urea and phosgene. The ligands were obtained after relatively short reaction times of 3–5 h in yields of 85–98%. Ligand **L2** has been identified previously in the gas phase by mass spectrometry but not isolated [28,29]. The characterization of the ligands was performed by NMR and IR spectroscopy as well as EI-MS analysis.

3.2. Dioxygen activation by copper(I) guanidine–amine-hybrid complexes

For investigation of the copper(I) guanidine–amine-hybrid complexes of **L1–L4** on their ability to activate oxygen the reaction of the in situ prepared Cu(I) guanidine solutions with oxygen at 195 K (THF, 1 atm O_2, [Cu] = 2 mM, PF_6^- and $CF_3SO_3^-$) was followed by UV–Vis spectroscopy. The UV–Vis spectra of the formed bis(μ-oxo) dicopper complexes are shown in Fig. 3. The oxygenated copper complex of **L2** has two intense charge transfer (CT) bands at 285 nm ($\varepsilon \approx 19$ mM^{-1} cm^{-1}) and 390 nm ($\varepsilon \approx 12$ mM^{-1} cm^{-1}) and a shoulder at ~450 nm ($\varepsilon \approx 8$ mM^{-1} cm^{-1}, Fig. 3) similar to those in $[Cu_2(TMGdmap)_2(\mu\text{-}O)_2](CF_3SO_3)_2$ (λ [nm]/ε [mM^{-1} cm^{-1}]: 297/20, 385/18, 430/8) [25]. This supports its composition as an bis(μ-oxo) species. For the guanidine–amine-hybrid ligands **L1**, **L3** and **L4**, no Cu_2O_2 species could be observed in the reaction of the corresponding Cu(I) precursor complexes with molecular oxygen, as the resulting UV–Vis spectra showed no characteristic CT bands for a Cu_2O_2 species (Fig. 3). Change of counterion did not lead to better formation of any Cu_2O_2 species. Up to now, it is not clear why **L1**,

Table 1
Crystal data for compounds **1**–**10**.

	1	**2**	**3**	**4**	**5**
Empirical formula	$C_{18}H_{42}Cu_2I_2N_8O_2$	$C_{20}H_{42}Cu_2F_6N_8O_8S_2$	$C_{18}H_{42}Cu_2F_{12}N_8O_2Sb_2$	$C_{18}H_{42}Cu_2F_{12}N_8O_2P_2$	$C_{18}H_{46}Cu_2I_2N_8O_2$
Molecular mass	783.48	827.82	1001.18	819.62	787.51
Crystal system	monoclinic	triclinic	triclinic	triclinic	monoclinic
Space group	$P2_1/n$	$P\bar{1}$	$P\bar{1}$	$P\bar{1}$	$P2_1/n$
a (Å)	8.776(1)	8.282(2)	8.7120(12)	8.405(1)	8.5523(11)
b (Å)	10.353(1)	9.110(2)	9.3260(13)	9.043(1)	16.8715(19)
c (Å)	16.235(2)	11.582(2)	11.0804(15)	11.010(1)	10.5365(16)
α (°)	90	88.721(4)	88.254(3)	88.392(2)	90
β (°)	103.514(3)	82.789(4)	79.933(3)	79.370(2)	93.515(3)
γ (°)	90	69.471(4)	67.579(2)	69.756(2)	90
V (Å^3)	1434.1(3)	811.7(3)	818.7(2)	771.03(16)	1517.5(3)
Z	2	1	1	1	2
R_1 $[I > 2\sigma(I)]$	R_1 = 0.0243,	R_1 = 0.0372,	R_1 = 0.0306,	R_1 = 0.0363,	R_1 = 0.0378,
wR_2 (all data)	wR_2 = 0.0621	wR_2 = 0.1017	wR_2 = 0.0818	wR_2 = 0.1004	wR_2 = 0.0795
	6	**7**	**8**	**9**	**10**
Empirical formula	$C_{20}H_{46}Cu_2F_6N_8O_8S_2$	$C_{22}H_{54}Cu_4I_4N_8O_2$	$C_{32}H_{62}Cu_2F_6N_8O_8S_2$	$C_{30}H_{62}Cu_2F_{12}N_8O_2Sb_2$	$C_{30}H_{62}Cu_2F_{12}N_8O_2P_2$
Molecular mass	831.85	1224.49	992.08	1165.46	983.9
Crystal system	monoclinic	monoclinic	triclinic	triclinic	monoclinic
Space group	$P2_1/n$	$P2_1/c$	$P\bar{1}$	$P\bar{1}$	$P2_1/c$
a (Å)	12.433(5)	10.093(2)	9.255(2)	9.465(4)	10.724(1)
b (Å)	9.330(3)	17.394(3)	10.756(2)	10.797(5)	9.360(1)
c (Å)	15.138(6)	11.041(2)	11.847(2)	11.807(5)	20.359(2)
α (°)	90	90	66.623(4)	66.249(6)	90
β (°)	103.262(7)	100.162(3)	84.078(4)	79.686(8)	90.635(2)
γ (°)	90	90	81.285(4)	77.721(8)	90
V (Å^3)	1709.2(11)	1907.9(5)	1068.8(4)	1073.3(8)	2043.5(4)
Z	2	2	1	1	2
R_1 $[I > 2\sigma(I)]$	R_1 = 0.0425,	R_1 = 0.0200,	R_1 = 0.0422,	R_1 = 0.0567,	R_1 = 0.0332,
wR_2 (all data)	wR_2 = 0.1046	wR_2 = 0.0471	wR_2 = 0.1156	wR_2 = 0.1474	wR_2 = 0.0880

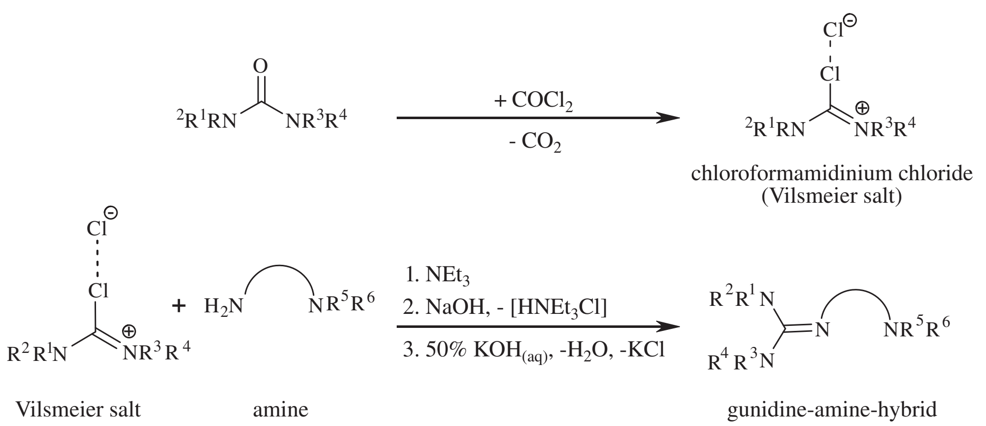

Fig. 2. Synthesis of guanidine–amine-hybrid ligands.

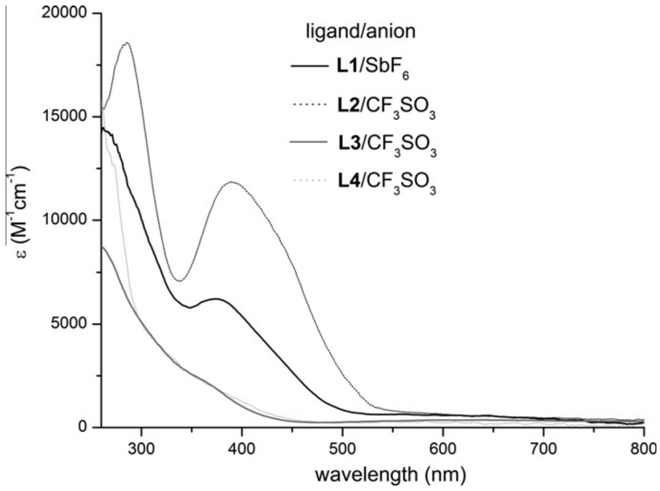

Fig. 3. UV–Vis spectra of the oxygenation products of the Cu(I) precursor complexes of **L1**–**L4**.

L3 and **L4** do not support Cu_2O_2 species on the minute time scale. It may be proposed that the ethylene spacer allows the competitive formation of bis(chelate) copper species. To clarify this point, further investigations such as stopped flow measurements are planned. The occurring color change (yellow → greenish blue) during the reaction indicates that the resulting reaction products are Cu(II) species. During the oxygenation of the Cu(I) precursor complexes undefined reactions take place and for their determination crystallographic characterization of the Cu(I) precursor complexes and the end products are required.

3.3. Synthetic aspects of the bis(μ-hydroxo)dicopper(II) guanidine–amine-hybrid complexes

Bis(μ-hydroxo)dicopper(II) guanidine–amine-hybrid complexes can be obtained on different synthesis routes. One synthetic possibility is the thermal decomposition of Cu_2O_2 complexes to form bis(μ-alkoxo) and bis(μ-hydroxo) complexes in a 1:1 ratio (Scheme 2a). This decomposition reaction of bis(μ-oxo)dicopper(III) complexes can be observed with UV–Vis spectroscopy (decrease of the band at 400 nm, see also [25]) and can be seen visually on the color changes from red to green, blue or purple. Monocrystalline products can be obtained by slow evaporation of the solvent of the reaction mixture. The same products are obtained by reaction of a in situ prepared Cu(I)-precursor solution with O_2 at 298 K (Scheme 2a). They can be isolated in crystalline form by gas phase diffusion of diethyl or diisopropyl ether. Due to the previous work of Schneider and Herres-Pawlis [16,33,34] on the related bisguanidine complexes for the guanidine–amine-hybrid systems a 1:1 mixture of bis(μ-alkoxo) and bis(μ-hydroxo)dicopper complex is expected as well. So far, for the guanidine–amine hybrid ligands only the bis(μ-hydroxo)dicopper complex could be isolated and structurally characterized. An indication for the simultaneous formation of the hydroxo and alkoxo form is the fact that in some cases two different crystallization products could be obtained. One example is the reaction of [Cu(DMEGdmae)I] with O_2 at 298 K, in which by gas-phase diffusion of diisopropyl blue squares and violet needles could be isolated in a crystalline form. But only the purple crystals could be characterized crystallographically and were identified as $[Cu_2(DMEGdmae)_2(\mu\text{-}OH)_2]I_2$ (**1**). The blue crystals were not stable enough to be prepared for X-ray crystallography. For this intramolecular monooxygenation reaction the maximum yield for the bis(μ-hydroxo) dicopper complex is 50%.

The other possibility is the reaction of the Cu(I) precursor complex with O_2 in the presence of atmospheric moisture at 298 K in THF leading to the bis(μ-hydroxo) dicopper complex in almost quantitative yields (80–90%) (Scheme 2b). Apparently with this type of reaction no formation of a bis(μ-alkoxo) species can be observed. The reason for this is an intermolecular monooxygenation reaction, in which THF acts as exogenous substrate. The oxidation of THF to 2-hydroxytetrahydrofuran by Cu_2O_2 species was already described in the literature. On the basis of ^{18}O-labeling experiments it could be shown that the O atom in the 2-hydroxytetrahydrofuran originates from the Cu_2O_2 species [35–38].

3.4. Crystal structures of bis(μ-hydroxo) dicopper(II) guanidine–amine-hybrid complexes

3.4.1. Crystal structures of bis(μ-hydroxo) dicopper complexes with DMEG function

For the reaction of the guanidine–amine-hybrid ligand DMEGdmae (**L1**) with different Cu (I) salts (CuI, $[Cu(MeCN)_4]CF_3SO_3$, $[Cu(MeCN)_4]SbF_6$, $[Cu(MeCN)_4]PF_6$) and subsequent reaction with O_2 the following bis(μ-hydroxo) dicopper complex could be isolated in crystalline form: $[Cu_2(DMEGdmae)_2(\mu\text{-}OH)_2]I_2$ (**1**), $[Cu_2(DMEGdmae)_2(\mu\text{-}OH)_2](CF_3SO_3)_2$ (**2**), $[Cu_2(DMEGdmae)_2(\mu\text{-}OH)_2](SbF_6)_2$ (**3**) and $[Cu_2(DMEGdmae)_2(\mu\text{-}OH)_2](PF_6)_2$ (**4**). The complex salt **1** crystallizes monoclinic in the space group $P2_1/n$ and the complex salts **2**–**4** crystallize triclinic in the space group $P\bar{1}$. All four compounds contain the complex cation $[Cu_2(DMEGdmae)_2(\mu\text{-}OH)_2]^{2+}$ with different anions for charge compensation. This series of bis(μ-hydroxo) dicopper complexes (**1**–**4**) allows to

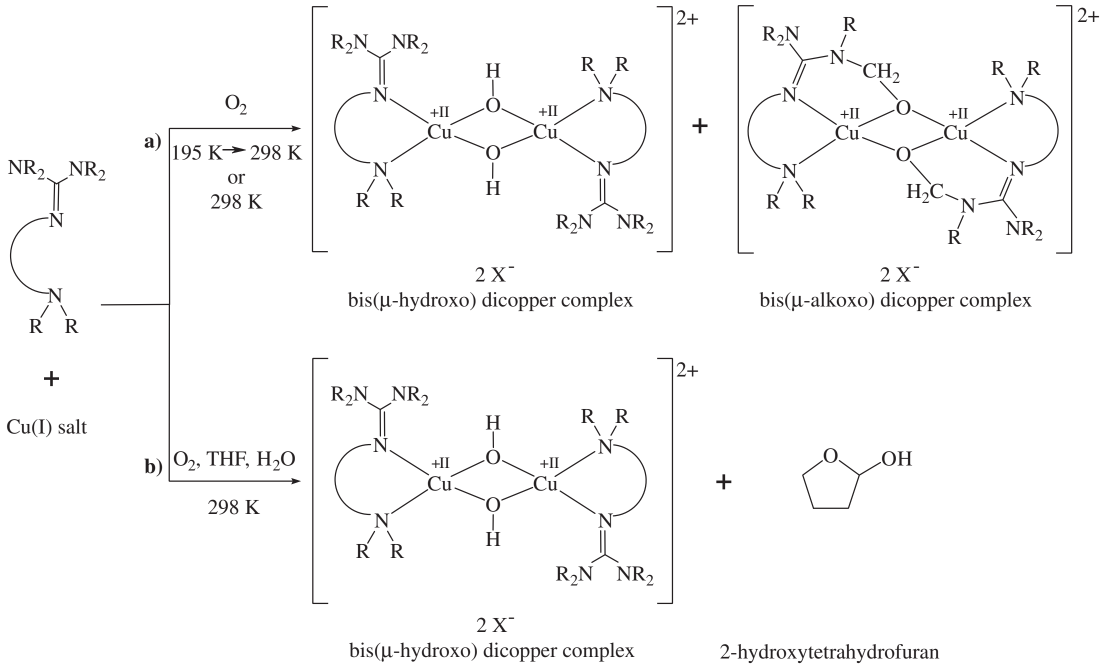

Scheme 2. General reaction scheme for the synthesis of bis(μ-hydroxo) dicopper(II) guanidine–amine-hybrid complexes.

investigate to which extent the structure of the complexes in the crystal is influenced by the anions. The Cu(II) ions of the four complexes are coordinated by a N_2O_2 donor set in a distorted square-planar manner, in which the central Cu_2O_2 core forms a rhomb with a central inversion center. The two chelating ligands are in *anti* position to each other. The molecular structure of the complex cation $[Cu_2(DMEGdmae)_2(\mu\text{-}OH)_2]^{2+}$ is shown in Fig. 4 using the example of **1**, selected bond lengths and angles are summarized in Table 2.

The bite angle N–Cu–N of the ligand DMEGdmae with an average of 85.1° (85.35(8)° **1**, 84.48(8)° **2**, 85.3(6)° **3**, 85.2(4)° **4**) and the relatively sharp O–Cu–O bond angle with an average of 82.4° (84.49(7)° **1**, 82.86(7)° **2**, 80.1(6)° **3**, 82.0(3)° **4**) leads to a slight distortion of the square-planar coordination geometry (ideal value 90°). The inverse rotation of the two CuN_2 planes against the central Cu_2O_2 plane about 11.9° (**1**), 4.1° (**2**), 5.7° (**3**) and 7.7° (**4**) also leads to a minimal deviation from planarity within the N_2CuO_2 unit. This torsion is also reflected in the sum of the environment angles for the two copper ions, which is with 705.0° (**1**), 713.1° (**2**), 709.7° (**3**) and 710.1° (**4**) slightly reduced from the ideal value of a square-planar geometry (720°). It is striking that the values of the N_{amine}–Cu–O, O–Cu–O′ and Cu–O–Cu′ angles in **1** (91.99(7)°/167.64(7)°, 84.49(7)° and 95.51(7)°) are significantly different from those of the complexes **2**–**4** (average 94.3°/173.2°, 81.7° and 98.3°). Due to the different Cu–O–Cu′ angles, the Cu···Cu′ distances of the four complexes also differ significantly from each other (see Table 2). Remarkable is the short Cu···Cu′ distance of 2.860(1) Å in **1**, which is

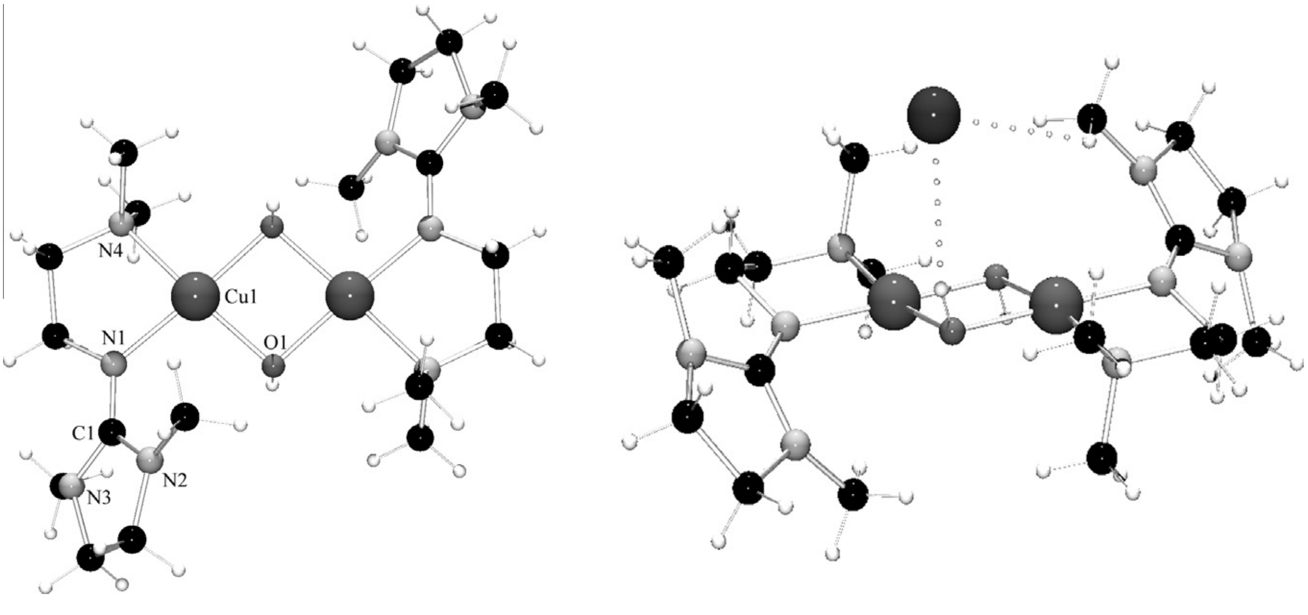

Fig. 4. Molecular structure of $[Cu_2(DMEGdmae)_2(\mu\text{-}OH)_2]^{2+}$ in crystals of **1** (left: frontal view, right: view with H bonds to iodine atoms).

Table 2
Selected structural data of **1**–**4**.

	1 $[Cu_2(DMEGdmae)_2(\mu\text{-}OH)_2]I_2$	**2** $[Cu_2(DMEGdmae)_2(\mu\text{-}OH)_2](CF_3SO_3)_2$	**3** $[Cu_2(DMEGdmae)_2(\mu\text{-}OH)_2](SbF_6)_2$	**4** $[Cu_2(DMEGdmae)_2(\mu\text{-}OH)_2](PF_6)_2$
Distances [Å]				
Cu···Cu′	2.860(1)	2.909(1)	2.944(4)	2.912(2)
Cu–O	1.935(2)	1.931(2)	1.930(13)	1.919(7)
Cu–O′	1.928(2)	1.949(2)	1.914(12)	1.940(8)
$Cu–N_{Imine,gua}$	1.961(2)	1.969(2)	1.947(13)	1.939(9)
$Cu–N_{Amine}$	2.031(2)	2.068(2)	2.034(15)	2.045(9)
$C_{gua}–N_{Imine,gua}$	1.308(3)	1.313(3)	1.31(2)	1.308(13)
$C_{gua}–N_{Amine,gua}$	1.345(3) 1.374(3)	1.358(3) 1.387(3)	1.36(2)1.37(2)	1.364(13) 1.372(13)
Angles [°]				
N–Cu–N	85.35(8)	84.48(8)	85.3(6)	85.2(4)
$N_{Imine,gua}–Cu–O$	98.25(7) 177.27(8)	98.64(8) 177.25(8)	99.8(6) 177.3(6)	98.7(3) 178.9(3)
$N_{Amine}–Cu–O$	91.99(7) 167.64(7)	94.15(7) 175.69(7)	94.6(5) 172.6(6)	94.0(3) 171.3(3)
O–Cu–O′	84.49(7)	82.86(7)	80.1(6)	82.0(3)
Cu–O–Cu′	95.51(7)	97.14(7)	99.9(6)	98.0(3)
Structural parameter (ρ)	0.96	0.96	0.96	0.96
Dihedral angle [°]				
$\angle(CuN_2, Cu_2O_2)$	11.9(1)	4.1(1)	5.7(7)	7.7(3)
$\angle(C_{gua}N_3,CuN_2)$	40.4(1)	49.5(1)	45.9(5)	46.8(2)
$\angle(N_{Amine,gua}C_3,C_{gua}N_3)$	13.1(av)	16.1(av)	15.4(av)	16.1(av)

significantly shorter than that in **2**–**4** and other bis(μ-hydroxo) dicopper complexes reported elsewhere [39–50]. Only three bis(μ-hydroxo) species which have similar short Cu···Cu′ distances (2.847 [45], 2.871 [46], 2.892 Å [46]) as **1** have been described so far, but in contrast to **1** these are stabilized by aromatic ligand systems.

The differences in the geometric parameters of the complex salts **1**–**4** can be explained by the position of the anions Y in the crystal, because they form hydrogen bonds to the OH functions of the complex cations (H···Y distances: 2.698 (**1**), 2.768 (**2**), 2.098 (**3**) and 2.204 Å (**4**)) and thereby easily influence the structure of bis(μ-hydroxo) species. Here, it is remarkable that the compound with the shortest H-bridge has the longest Cu···Cu′ distance (2.944(4) Å **3**).

Another bis(μ-hydroxo)dicopper complex with ethylene bridged guanidine functions represents the complex $[Cu_2(BL^{iPr})_2(\mu\text{-}OH)_2](PF_6)_2$ **11** [39], which contains two imidazoline based bisguanidine ligands. Besides this bis(μ-hydroxo) dicopper guanidine complex in the literature numerous bis(μ-hydroxo) species with ethylene bridged nitrogen chelate ligands have been described. The main structural data of the bis(μ-hydroxo) dicopper complex $[Cu_2(BL^{iPr})_2(\mu\text{-}OH)_2](PF_6)_2$ **11** [39], $[Cu_2(Me_2en)_2(\mu\text{-}OH)_2](X)_2{\cdot}nH_2O$ ($X^-/n = ClO_4^-/2$ **12a** [40], $BF_4^-/0$ **12b** [41], $Br^-/0$ **12c** [42]), $[Cu_2(DBED)_2(\mu\text{-}OH)_2](BF_4)_2$ **13** [43], $[Cu_2(d^{cis}d)_2(\mu\text{-}OH)_2](CF_3SO_3)_2$ **14** [44], $[Cu_2(bpp)_2(\mu\text{-}OH)_2](ClO_4)_2$ **15** [45] and $[Cu_2(bipy)_2(\mu\text{-}OH)_2](X)_2$ ($X^- = ClO_4^-$ **16a** [46], $CF_3SO_3^-$ **16b** [47]) are summarized in Table 3, the schematic structures of these compounds are shown in Fig. 5.

A comparison of the structures **1–4** with the known compounds shows a good agreement between the average Cu-O distances of **1–4** (1.922–1.940 Å) with **11**, **15** and **16** (1.918–1.931 Å). The average Cu–O distances of **12**, **13** and **14** (1.898–1.913 Å), however, are slightly shorter, because they contain weaker N-donors. The average Cu–N distance in **11** (1.933 Å) corresponds to that of the $Cu–N_{imine,gua}$ distances in **1–4** (1.939–1.969 Å), as the $N_{imine,gua}$ donor strength of the coordinating bis(imidazolin-2-imine) ligand is comparable with that of the guanidine–amine-hybrid. The average Cu–N distances in **12–16** (1.990–2.034 Å) are due to the lower donor strength of the coordinating ligands much longer and thus match well with the longer $Cu–N_{Amine}$ distances in **1–4**

Table 3
Selected structural data of **11**–**21**.

Complex	Distances [Å]			Angles [°]			Coordination geometry[b]	Ref.
	Cu···Cu′	Cu–O[a]	Cu–N[a]	N–Cu–N	O–Cu–O′	Cu–O–Cu′		
11	3.049(1)	1.931	1.933	84.52(8)	75.72(8)	104.28(8)	d.q.-p.	[39]
12a	2.976(1)	1.913	2.034	86.7(2)	77.9(2)	102.14	d.q.-p.	[40]
12b	2.996(1)	1.911	2.010	87.28(7)	76.77(8)	103.23(8)	d.q.-p.	[41]
12c	3.000(4)	1.902	2.030	86.7(8)	75.92(17)	104.08(17)	d.q.-p.	[42]
13	2.972(1)	1.908	2.009	88.5[a]	77.7[a]	102.3[a]	d.t.	[43]
14	2.972(2)	1.898	2.024	85.7[a]	77.0[a]	103.0(4)	d.q.-p.	[44]
15	2.847(1)	1.926	2.008	80.5[a]	84.6[a]	95.4[a]	d.q.-p.	[45]
16a	2.871(1)	1.918	1.990	81.58(11)	83.06(14)	96.94(15)	d.q.-p.	[46]
16b	2.920(1)	1.927	1.996	81.5(2)	81.5(1)	98.5(1)	d.q.-p.	[47]
17	2.952(4)	1.929	2.013	90.5[a]	79.5[a]	99.2(10)	d.t.	[48]
18	3.014(1)	1.944	2.014	91.98(11)	78.32(12)	101.69(11)	d.q.-p.	[25]
19a	3.008(2)	1.944	1.987	94.0(2)	78.6(2)	101.4(2)	d.q.-p.	[16]
19b	3.032(1)	1.944	1.987	94.0(2)	78.6(2)	101.4(2)	d.q.-p.	[16]
20	3.074(1)	1.935	1.975	96.02(11)	74.78(11)	105.22(11)	d.q.-p.	[49]
21a	2.938(1)	1.942	2.037	94.95(8)	81.65(9)	98.35(8)	d.q.-p.	[43]
21b	2.949(1)	1.932	2.034	95.07(11)	80.50(9)	99.63(9)	d.q.-p.	[51]

[a] Average.
[b] d.q.-p. = distorted square-planar, d. t. = distorted tetrahedral

(2.031–2.068 Å). The O–Cu–O′ and Cu–O–Cu′ angle, as well as the Cu···Cu′ distances in **15** and **16** (81.5–84.6° and 95.4–98.5°, 2.847–2.920 Å) are comparable with those in **1–4** (80.1–84.5° and 95.5–99.9°, 2.860–2.944 Å). The Cu···Cu′ distances in **11–14** (2.972–3.049 Å), however, are significantly larger than that of the guanidine–amine-hybrid complexes.

Analogously to **1–4** the compounds **12c** and **16a–b** also represent a series of bis(μ-hydroxo) dicopper complexes that differ in composition only by the anions. However, **12a–c** and **16a–b**, show only slight differences in the bond lengths and angles within a series (see Table 3), so that the influence of the anions becomes only slightly noticeable. Furthermore, it is striking that the Cu(II) ions in **11**, **12** and **14–16** are surrounded in a distorted square-planar manner as well as in **1–4**, while the coordination geometry of the Cu(II) ion in **13** is distorted tetrahedral. This for bis(μ-hydroxo) dicopper complexes unusual tetrahedral coordination of Cu(II) ions has been observed only for one other bis(μ-hydroxo) species $[Cu_2(Sp)_2(\mu\text{-}OH)_2](ClO_4)_2$ **17** [48] so far, but this includes a propylene instead of an ethylene spacer (Fig. 5, Table 4).

3.4.2. Crystal structures of bis(μ-hydroxo) dicopper(II) complexes with TMG function

The reaction of Cu (I) precursor complexes obtained by reaction of TMGdmae (**L2**) and TMGdeae (**L3**) with CuI or $[Cu(MeCN)_4]CF_3SO_3$ with molecular oxygen leads to the corresponding bis (μ-hydroxo) reaction products, which could be isolated as single crystals with the composition $[Cu_2(TMGdmae)_2(\mu\text{-}OH)_2]I_2$ **5**, $[Cu_2(TMGdmae)_2(\mu\text{-}OH)_2](CF_3SO_3)_2$ **6** and $[Cu_2(TMGdeae)_2(\mu\text{-}OH)_2](Cu_2I_4)$ **7**. The complex salts **5–7** crystallize monoclinic in the space group $P2_1/n$ (**5, 6**) or $P2_1/c$ (**7**). The crystals of the three compounds consist of the dinuclear complex cations $[Cu_2(TMGdmae)_2(\mu\text{-}OH)_2]^{2+}$ (**5, 6**) or $[Cu_2(TMGdeae)_2(\mu\text{-}OH)_2]^{2+}$ (**7**) and charge-compensating iodide (**5**) triflate (**6**) or $[Cu_2I_4]^{2-}$ anions (**7**). The Cu(II) ions in **5–7** are each four-coordinate with two coordination sites occupied by the two N-donor functions of the corresponding guanidine–amine-hybrid ligands and two coordination sites occupied by the bridging hydroxido ligands, so that each Cu(II) ion is bound in an approximately square-planar N_2O_2 environment. The central Cu_2O_2 cores form a rhomb with a centric inversion

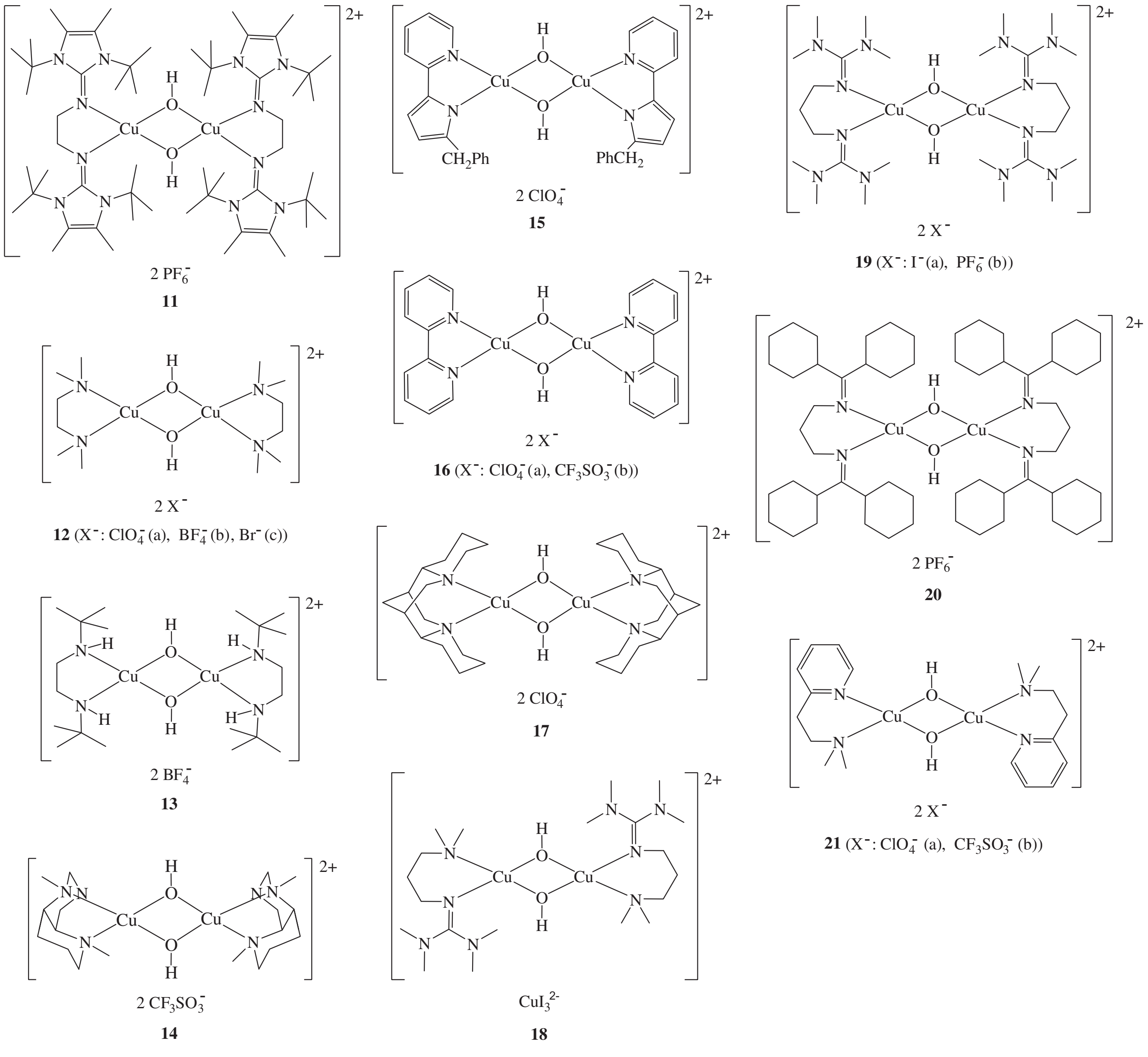

Fig. 5. Schematic structures of the bis(μ-hydroxo) dicopper complexes **11–21**.

Table 4
Selected structural data of **5**–**7**.

	5 $[Cu_2(TMGdmae)_2(\mu\text{-}OH)_2]I_2$	**6** $[Cu_2(TMGdmae)_2(\mu\text{-}OH)_2](CF_3SO_3)_2$	**7** $[Cu_2(TMGdeae)_2(\mu\text{-}OH)_2](Cu_2I_4)$
Distances [Å]			
Cu···Cu′	2.883(1)	2.901(1)	2.944(1)
Cu–O	1.932(2)	1.917(1)	1.927(2)
Cu–O′	1.948(2)	1.936(1)	1.967(2)
$Cu–N_{Imine,gua}$	1.949(3)	1.933(2)	1.933(2)
$Cu–N_{Amine}$	2.033(3)	2.037(2)	2.071(2)
$C_{gua}–N_{Imine,gua}$	1.311(4)	1.311(2)	1.316(3)
$C_{gua}–N_{Amine,gua}$	1.365(4)	1.355(3)	1.364(3)
	1.368(4)	1.357(2)	1.366(3)
Angles [°]			
N–Cu–N	84.90(11)	85.27(7)	85.21(7)
$N_{Imine,gua}–Cu–O$	98.52(10)	97.39(6)	96.71(7)
	176.73(11)	178.16(6)	176.40(7)
$N_{Amine}–Cu–O$	93.00(10)	94.81(6)	96.83(7)
	168.35(10)	171.63(6)	170.42(7)
O–Cu–O′	84.03(10)	82.28(6)	81.77(7)
Cu–O–Cu′	95.97(10)	97.72(6)	98.23(7)
Structural parameter (ρ)	0.96	0.97	0.96
Dihedral angle [°]			
$\angle(CuN_2, Cu_2O_2)$	11.7(1)	8.0(1)	10.3(1)
$\angle(C_{gua}N_3, CuN_2)$	42.4(1)	51.5(1)	51.1(1)
$\angle(N_{Amine,gua}C_3, C_{gua}N_3)$	35.9	34.4	34.9

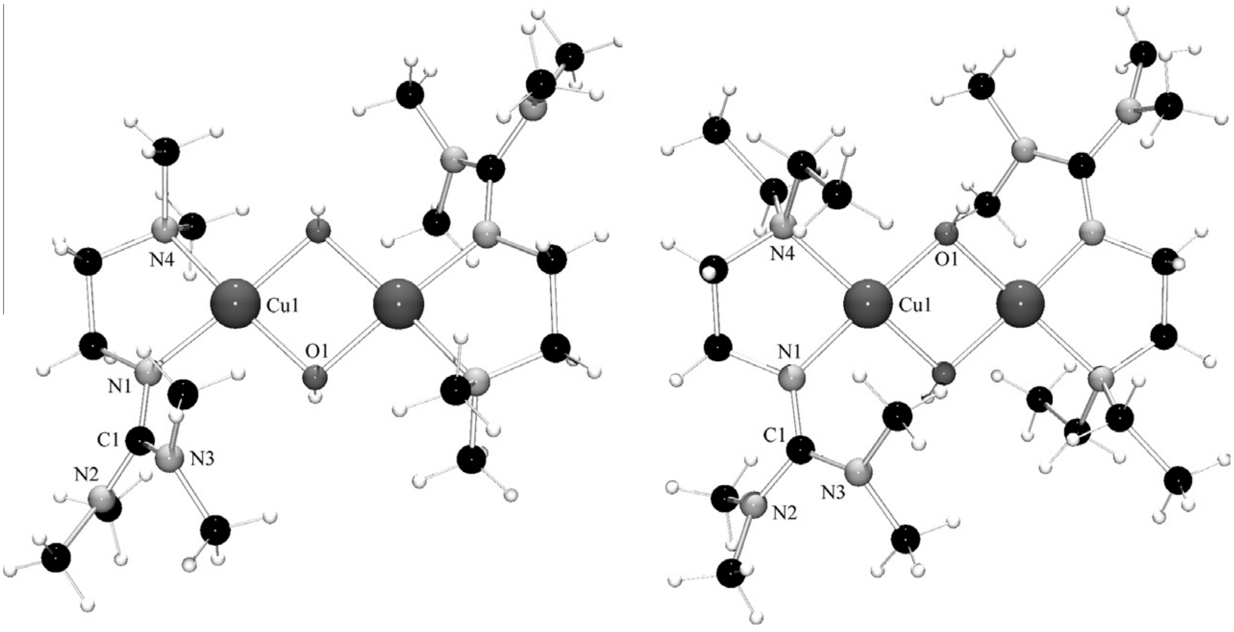

Fig. 6. Molecular structure of $[Cu_2(TMGdmae)_2(\mu\text{-}OH)_2]^{2+}$ (left) and $[Cu_2(TMGdeae)_2(\mu\text{-}OH)_2]^{2+}$ (right) in crystals of **5** and **7**.

center. Selected bond lengths and angles are given in Table 4, the molecular structure of the complex cations of **5** and **6** (using the example of **5**) and of **7** in the crystal are shown in Fig. 6.

An ideal square-planar coordination geometry of the Cu(II) ions in **5–7** is not possible because of the N–Cu–N bite angle of an average of 85.1° (84.90(11)° **5**, 85.27(7)° **6**, 85.21(7)° **7**) imposed by the ligands and the relatively sharp O–Cu–O angle of an average of 82.7° (84.03(10)° **5**, 82.28(6)° **6**, 81.77(7)° **7**).

Due to the torsion of the two CuN_2 planes against the central Cu_2O_2 plane about 11.7° (**5**), 8.0° (**6**) and 10.3° (**7**) there is also a slight deviation from planarity within the CuN_2O_2 unit, which is reflected in a slight distortion of the Cu(II) environment (angle sum: 705.8° (**5**), 709.5° (**6**) and 707.3° (**7**), ideal value: 720°). The average Cu–O bonds in **5** (1.940 Å) and **7** (1.947 Å) have approximately the same length, in **6** (1.927 Å), however, they are slightly shorter. The other bond lengths show no large differences (see Table 4). The dihedral angle for the torsion of the $C_{gua}N_3$ against the CuN_2 plane, however, differs significantly among the three complexes.

Furthermore for **5** and **6**, that differ in composition only by the anions, a slight influence of anions on the structure of the complexes in the crystal can be observed, because they show significant differences in Cu···Cu′ (2.883 (1) **5** vs. 2.901(1) Å **6**) and Cu–O distances (1.932(2)/1.948(2) **5** vs. 1.917(1)/1.936(1) Å **6**) as well as in the bond angles (see Table 4). The distances of the hydrogen bonds H···Y are 2.677 (**5**) and 2.063 Å (**6**), the compound with the shorter H-bridge also exhibits the longer Cu···Cu′ distance (2.901(1) Å **6**). In the complex salt **7** also H-bonds to the anions

Table 5
Selected structural data of **8**–**10**.

	8 [$Cu_2(DPipGdmae)_2(\mu\text{-}OH)_2](CF_3SO_3)_2$	**9** [$Cu_2(DPipGdmae)_2(\mu\text{-}OH)_2](SbF_6)_2$	**10** [$Cu_2(DPipGdmae)_2(\mu\text{-}OH)_2](PF_6)$
Distances [Å]			
Cu···Cu′	2.942(1)	2.952(2)	2.921(2)
Cu–O	1.911(2)	1.926(4)	1.945(5)
Cu–O′	1.933(2)	1.938(4)	1.907(5)
Cu–$N_{Imine,gua}$	1.937(2)	1.949(4)	1.931(6)
Cu–N_{Amine}	2.046(2)	2.038(4)	2.041(6)
C_{gua}–$N_{Imine,gua}$	1.325(3)	1.311(7)	1.315(9)
C_{gua}–$N_{Amine,gua}$	1.357(3)	1.352(7)	1.364(9)
	1.364(3)	1.359(7)	1.366(9)
Angles [°]			
N–Cu–N	85.64(7)	86.06(18)	85.4(2)
$N_{Imine,gua}$–Cu–O	99.49(7)	99.37(18)	97.7(2)
	178.60(7)	179.72(17)	177.7(2)
N_{Amine}–Cu–O	95.03(7)	94.20(17)	95.8(2)
	166.62(7)	168.83(19)	168.7(2)
O–Cu–O′	80.11(7)	80.38(19)	81.4(2)
Cu–O–Cu′	99.89(7)	99.62(17)	98.6(2)
Structural parameter (ρ)	0.97	0.97	0.96
Dihedral angle [°]			
$\angle(CuN_2, Cu_2O_2)$	12.8(1)	9.9(2)	11.4(4)
$\angle(C_{gua}N_3, CuN_2)$	40.4(1)	41.2(2)	46.9(3)
$\angle(N_{Amine,gua}C_3, C_{gua}N_3)$	32.3	38.2	34.1

are present, but with H···Y distances of 3.209 Å (**7**) they are much longer, so their influence on the structure of the complex is negligible. Compared with the corresponding complexes **1** and **2**, including a DMEG function, in particular the Cu···Cu distances and the bond angles are in good agreement; but also between **2–4** and **6–7** good agreements in bond lengths and angles can be found.

Another bis(μ-hydroxo) dicopper guanidine–amine-hybrid complex with a TMG function, which was published by us recently, is [$Cu_2(TMGdmap)_2(\mu\text{-}OH)_2](CuI_3)$ **18** [25]. In contrast to **5–7**, it possesses a propylene-spacer, resulting in a significantly larger bite angle (91.98(11)°), which is relatively similar to the ideal value of the square-planar geometry (90°). But also in this case the very sharp O–Cu–O bond angle of 78.32(12)° impedes a perfect square-planar coordination geometry. In addition, the contraction of the O–Cu–O angle in **18** due to the planarity of the central Cu_2O_2 units results in an expansion of the Cu–O–Cu angle (101.69(11)° vs. 95.97(10)° **5**, 97.72(6)° **6**, 98.23(7)° **7**) and hence an increase in the Cu···Cu distance (3.014(1) vs. 2.883(1) **5**, 2.901(1) **6**, 2.944 Å **7**). Further bis(μ-hydroxo) dicopper complexes with a propylene spacer $(CH_2)_3$ were described in the literature only rarely. Similar complexes to **18** are the known bisguanidine complexes [$Cu_2(btmgp)_2(\mu\text{-}OH)_2](X)_2$ ($X^- = I^-$ **19a**, PF_6^- **19b**) [16], [$Cu_2(DPipG_2p)_2(\mu\text{-}OH)_2](PF_6)_2$ **20** [49], the sparteine complex [$Cu_2(Sp)_2(\mu\text{-}OH)_2](ClO_4)_2$ **17** [48] and the dimethylamino ethyl pyridine complexes [$Cu_2(DMAEP)_2(\mu\text{-}OH)_2](X)_2$ ($X^- = ClO_4^-$ **21a** [43], $CF_3SO_3^-$ **21b** [51]). A comparison of the three structures **5–7** with the known compounds **11**–**16** (see Fig. 5 and Table 3) shows great similarities as the comparison of **1–4** with **11–16** (see above). It is remarkable that the Cu···Cu distance correlates with the length of the stabilizing hydrogen bonds which are formed between the hydroxide O atoms and the counterions. Short H···O distances go along with larger Cu···Cu distances. Especially in iodido stabilized bis(μ-hydroxo) dicopper complexes (e.g. complexes **1** and **5**), very short Cu···Cu distances are found.

3.4.3. Crystal structures of bis(μ-hydroxo) dicopper(II) complexes with DPipG function

The reaction of various Cu(I) precursor complexes [$Cu_m(\mathbf{L})_n]Y_m$ ($Y^- = CF_3SO_3^-$, SbF_6^-, PF_6^-) of DPipGdmae (**L4**) with O_2 leads to the bis(μ-hydroxo) dicopper complexes [$Cu_2(DPipGdmae)_2(\mu\text{-}OH)_2](CF_3SO_3)_2$ **8**, [$Cu_2(DPipGdmae)_2(\mu\text{-}OH)_2](SbF_6)_2$ **9** and [$Cu_2(DPipGdmae)_2(\mu\text{-}OH)_2](PF_6)_2$ **10**. All three complex salts contain the dinuclear complex cation [$Cu_2(DPipGdmae)_2(\mu\text{-}OH)_2]^{2+}$ with different anions for charge compensation. **8** and **9** crystallize triclinic in the space group $P\bar{1}$, **10** crystallizes monoclinic in space group $P2_1/c$. A summary of selected bond lengths and angles is given in Table 5, the molecular structure of the complex cation

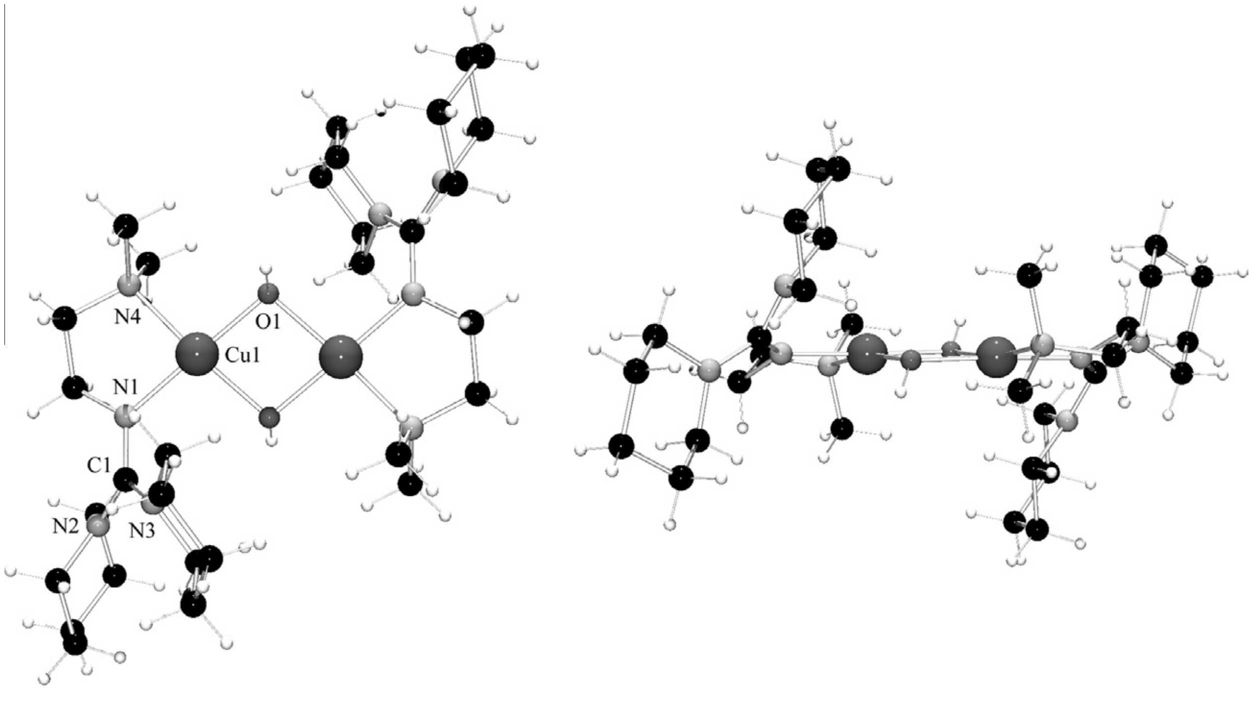

Fig. 7. Molecular structure of [$Cu_2(DPipGdmae)_2(\mu\text{-}OH)_2]^{2+}$ in crystals of **10** (left: frontal view, right: side view).

Table 6
Extraction of the literature overview: ranges of bond lengths and angles in bis(μ-oxo) and bis(μ-hydroxo) dicopper complexes (key parameters are marked in bold).

Complex type	Bis(μ-oxo) dicopper complexes		Bis(μ-hydroxo) dicopper complexes		Bis(μ-hydroxo) complexes of this work
Ligand type	Neutral	Anionic	Neutral	Anionic	Neutral
Cu–O (Å)	1.803–1.834	1.817–1.865	1.902–1.974	1.917–1.924	1.907–1.967
Cu–N (Å)	1.939–1.991	1.888–1.996	1.931–2.088	1.937–1.959	1.931–2.071
Sum$_{2cuo+2CuN}$ **(Å)**	**7.484–7.650**	**7.410–7.686**	**7.728–8.088**	**7.684–7.766**	**7.822–7.917**
Cu···Cu (Å)	**2.744–2.866**	**2.849–2.906**	**2.782–3.074**	**2.981–3.058**	**2.860–2.952**
O···O (Å)	2.287–2.334	2.258–2.338	2.342–2.592	2.331–3.318	2.473–2.622
N–Cu–N (°)	86.9–99.2	77.4–98.8	72.1–96.6	88.1–95.3	84.5–86.1
O–Cu–O (°)	77.2–80.7	76.8–77.6	74.8–84.6	74.3–76.6	80.1–84.5
sum$_{NCuN,OCuO}$ (°)	**167.1–176.4**	**155.0–175.6**	**150.6–178.1**	**164.3–170.7**	**165.4–169.8**
Cu–O–Cu	99.2–102.8	102.4–103.2	89.3–105.7	102.1–105.7	95.5–99.9

$[Cu_2(DPipGdmae)_2(\mu\text{-}OH)_2]^{2+}$ is shown in Fig. 7 using the example of **10**.

In all three complex cations the Cu(II) ions are coordinated by a N_2O_2 donor set in a distorted square-planar manner, the chelating ligands are in *anti* position to each other. The central Cu_2O_2 cores form a rhomb with a central inversion center. The average Cu–O bond lengths in **8–10** (1.922 **8**, 1.932 **9**, 1.926 Å **10**) show no large differences. The Cu···Cu′ distances in **8** (2.942(1) Å) and **9** (2.952(2) Å) have approximately the same length, the Cu···Cu′ distance in **10** (2.921(2) Å), however, is slightly shorter. An ideal square-planar coordination geometry of Cu(II) ions is not possible due to the bite angle N–Cu–N with an average of 85.7° (85.64(7)° **8**, 86.06(18)° **9**, 85.4(2)° **10**) and the relatively sharp O–Cu–O bond angle with an average of 80.6° (80.11(7)° **8**, 80.38(18)° **9**, 81.4(2)° **10**), so that a slight distortion occurs. The torsion of the two CuN_2 planes against the central Cu_2O_2 plane of 12.8° (**8**), 9.9° (**9**) and 11.4° (**10**) leads to a minimal deviation from planarity within the N_2CuO_2 unit. This is also reflected by the sum of environment angles of the Cu(II) ions, which are with 705.5° (**8**), 708.6° (**9**) and 706.4° (**10**) slightly decreased compared with the ideal value for a square-planar geometry (720°).

All other bond lengths and angles of the three complexes show no big differences and agree relatively well with the values in **1–7**. Hydrogen bonds between the anion to the proton of the OH ligands are only in **9** (F···H = 2.097 Å) and **10** (F···H = 2.050 Å) present. A significant influence of different anions can not be observed here.

An important feature of guanidines is the charge delocalization within the CN_3 unit. Hence, the lengths of the formal double C=N bond and the formal C–NR_2 single bonds are levelled. For the evaluation of the elongation of the C=N double bond and the shortening of the C–NR_2 bonds within the guanidine unit, the ρ value was introduced by Sundermeyer and co-workers [52]. It is calculated by the formula $\rho = 2a/(b + c)$ wherein a is the C=N bond length and b and c are the C–NR_2 bond lengths. In the case of a C_3-symmetrical CN_3 unit ρ is equal to 1. In all complexes reported herein, the parameter ρ ranges between 0.96 and 0.97 indicating a good delocalization typical for copper(II) complexes.

3.5. Literature overview on structurally characterized bis(μ-oxo) and bis(μ-hydroxo) dicopper(II) complexes

Due to the structural characterization of complex **1** with the very short Cu···Cu distance of 2.860(1) Å, the question arose which Cu···Cu distances still characterize a bis(μ-hydroxo) complex and if there is a typical bond length range usable for identification of such complexes. In some cases the H atoms cannot be located in the complex structure and then, such a classification can be useful. Hence, we performed a CSD research on bis(μ-oxo) dicopper complexes and bis(μ-hydroxo) dicopper(II) complexes with bidentate ligands and differentiated them for the incorporated type of ligand. Anionic ligands bind stronger to the copper centers as neutral ligands which results in longer Cu–O bonds for complexes with anionic ligands. An analysis of the structural data of known bis(μ-oxo) and bis(μ-hydroxo) complexes is summarized in Table 6. This analysis shows that compounds with Cu–O, Cu–N and Cu···Cu distances in the range of 1.803–1.865, 1.888–1.996 and 2.744–2.906 Å are more likely to be bis(μ-oxo) dicopper complexes, while compounds with Cu–O, Cu–N and Cu···Cu distances of 1.900–1.974, 1.931–2.088, 2.782–3.074 Å are more likely to be bis(μ-hydroxo) dicopper complexes (see Supporting information, Tables A1–A16). The Cu···Cu distance ranges for bis(μ-oxo) and bis(μ-hydroxo) dicopper complexes with neutral ligands widely overlap and cannot be used as single criterion for classification. For this reason, we calculated the sum of the bond lengths within the Cu_2O_2 rhomb and the sum of the angles in this rhomb. By using the bond length sum, it can be clearly distinguished between bis(μ-oxo) and bis(μ-hydroxo) dicopper complexes with neutral ligands: in bis(μ-oxo) complexes, this sum ranges from 7.484 to 7.650 Å whereas bis(μ-hydroxo) complexes display a sum range from 7.728 to 8.088 Å. The complexes reported herein fit exactly in this range although they differ in specific bond lengths or angles from other bis(μ-hydroxo) dicopper complexes.

4. Conclusion

In this contribution, new bidentate guanidine–amine hybrid ligands are presented. Their copper (I) complexes react with dioxygen, but only in case of **L2**, a defined Cu_2O_2 species could be observed to be a bis(μ-oxo) dicopper species. Ethylene spacers in guanidine–amine ligands seem not to be favorable for the formation of stable low-temperature Cu_2O_2 species. The subsequent reactions allowed the isolation and structural characterization of numerous bis(μ-hydroxo) dicopper(II) complexes. In all ten complexes, the copper(II) ion resides in a distorted square-planar environment and the N donor ligands are arranged in *anti* position to each other. The complex $[Cu_2(DMEGdmae)_2(\mu\text{-}OH)_2]I_2$ exhibits a Cu···Cu distance of 2.860(1) Å, which is one of the smallest observed for hydroxo-bridged copper compounds so far. The Cu···Cu distance correlates with the length of the stabilizing hydrogen bonds which are formed between the hydroxide O atoms and the counterions. Short H···O distances go along with larger Cu···Cu distances. Especially in bis(μ-hydroxo) dicopper complexes with iodide as anion, short Cu···Cu distances are found.

In a literature overview of structurally characterized bis(μ-oxo) and bis(μ-hydroxo) dicopper complexes, the structural features of such complexes could be highlighted: the most important factors are the type of ligand (anionic or neutral), the coordinative ability of the charge compensating anion and the bite angle imposed by the ligand. It is remarkable that the range of the Cu···Cu distance in bis(μ-oxo) and bis(μ-hydroxo) dicopper complexes overlap to a great extent, but by using the sum of the copper surrounding bond lengths, a classification is easily possible.

Acknowledgements

We gratefully acknowledge the financial support of the Fonds der Chemischen Industrie and of the Deutsche Akademische Austauschdienst DAAD (fellowships for S. H.-P.). R.H. thanks the Evonik Stiftung for granting a Ph.D. fellowship. S.H.-P. thanks Prof. K. Jurkschat and Prof. T.D.P. Stack for their valuable support.

Appendix A. Supplementary material

CCDC 810217–810226 contain the supplementary crystallographic data for compounds **1**–**10**, respectively. These data can be obtained free of charge from The Cambridge Crystallographic Data Centre via http://www.ccdc.cam.ac.uk/data_request/cif. Supplementary data associated with this article can be found, in the online version, at doi:10.1016/j.ica.2011.02.061.

References

[1] K.D. Karlin, Z. Tyeklár (Eds.), Bioinorganic Chemistry of Copper, Chapman and Hall, New York, 1993.
[2] N. Kitajima, Y. Moro-oka, Chem. Rev. 94 (1994) 737.
[3] J.A. Halfen, S. Mahapatra, E.C. Wilkinson, S. Kaderli, V.G. Young Jr., L. Que Jr., A.D. Zuberbühler, W.B. Tolman, Science 271 (1996) 1397.
[4] E.I. Solomon, U.M. Sundaram, T.E. Machonkin, Chem. Rev. 96 (1996) 2563.
[5] W.B. Tolman, Acc. Chem. Res. 30 (1997) 227.
[6] P.L. Holland, W.B. Tolman, Coord. Chem. Rev. 192 (1999) 855.
[7] S. Schindler, Eur. J. Inorg. Chem. (2000) 2311.
[8] V. Mahadevan, M.J. Henson, E.I. Solomon, T.D.P. Stack, J. Am. Chem. Soc. 122 (2000) 10249.
[9] A.G. Blackman, W.B. Tolman, Struct. Bond. 97 (2000) 179.
[10] V. Mahadevan, R.J.M. Klein Gebbink, T.D.P. Stack, Curr. Opin. Chem. Biol. 4 (2000) 228.
[11] E.I. Solomon, P. Chen, M. Metz, S.-K. Lee, A.E. Palmer, Angew. Chem. 113 (2001) 4702 (Angew. Chem., Int. Ed. 40 (2001) 4570).
[12] T.D.P. Stack, J. Chem. Soc., Dalton Trans. 10 (2003) 1881.
[13] E.A. Lewis, W.B. Tolman, Chem. Rev. 104 (2004) 1047.
[14] L.M. Mirica, X. Ottenwaelder, T.D.P. Stack, Chem. Rev. 104 (2004) 1013.
[15] H.-C. Liang, M.J. Henson, L.Q. Hatcher, M.A. Vance, C.X. Zhang, D. Lahti, S. Kaderli, R.D. Sommer, A.L. Rheingold, A.D. Zuberbühler, E.I. Solomon, K.D. Karlin, Inorg. Chem. 43 (2004) 4115.
[16] S. Herres, A.J. Heuwing, U. Flörke, J. Schneider, G. Henkel, Inorg. Chim. Acta 358 (2005) 1089.
[17] S. Herres-Pawlis, U. Flörke, G. Henkel, Eur. J. Inorg. Chem. (2005) 3815.
[18] L.M. Mirica, M. Vance, D.J. Rudd, B. Hedman, K.O. Hodgson, E.I. Solomon, T.D.P. Stack, Science 308 (2005) 1890.
[19] L.Q. Hatcher, K.D. Karlin, Adv. Inorg. Chem. 58 (2006) 131.
[20] L.M. Mirica, D.J. Rudd, M.A. Vance, E.I. Solomon, K.O. Hodgson, B. Hedman, T.D.P. Stack, J. Am. Chem. Soc. 128 (2006) 2654.
[21] S. Itoh, Y. Tachi, J. Chem. Soc., Dalton Trans. (2006) 4531.
[22] S. Itoh, S. Fukuzumi, Acc. Chem. Res. 40 (2007) 592.
[23] A. Company, S. Palavicini, I. Garcia-Bosch, R. Mas-Ballesté, L. Que Jr., E.V. Rybak-Akimova, L. Casella, X. Ribas, M. Costas, Chem.-Eur. J. 14 (2008) 3535.
[24] A. De, R. Mukherjee, J. Inorg. Biochem. 102 (2008) 1170.
[25] S. Herres-Pawlis, P. Verma, R. Haase, P. Kang, C.T. Lyons, E.C. Wasinger, U. Flörke, G. Henkel, T.D.P. Stack, J. Am. Chem. Soc. 131 (2009) 1154.
[26] I. Garcia-Bosch, A. Company, J.R. Frisch, M. Torrent-Sucarrat, M. Cardellach, I. Gamba, M. Güell, L. Casella, L. Que Jr., X. Ribas, J.M. Luis, M. Costas, Angew. Chem. 122 (2010) 2456 (Angew. Chem., Int. Ed. 49 (2010) 2406).
[27] R. Haase, Dissertation, Universität Paderborn, 2010.
[28] E.D. Raczyńska, M. Decouzon, J.-F. Gal, P.-C. Maria, G. Gelbard, F. Vielfaure-Joly, J. Phys. Org. Chem. 14 (2001) 25.
[29] (a) JP 2002 148749 A (2004).;
(b) US 005637439 A (1997).;
(c) DE 19541460 A 19960509(1996).
[30] SMART (Version 5.62), Bruker AXS Inc., Madison, WI, 2002.
[31] G.M. Sheldrick, Acta Crystallogr., A 64 (2008) 112.
[32] W. Kantlehner, E. Haug, W.W. Mergen, P. Speh, T. Maier, J.J. Kapassakalidis, H.-J. Bräuner, H. Hagen, Liebigs Ann. Chem. 1 (1984) 108.
[33] S. Herres-Pawlis, Dissertation, Universität Paderborn, 2005.
[34] J. Schneider, Dissertation, Universität Duisburg, 2000.
[35] Y. Kajita, H. Arii, T. Saito, Y. Saito, S. Nagatomo, T. Kitagawa, Y. Funahashi, T. Ozawa, H. Masuda, Inorg. Chem. 46 (2007) 3322.
[36] C. Xin Zhang, H.-C. Liang, E.-i. Kim, J. Shearer, M.E. Helton, Eunsuk Kim, S. Kaderli, C.D. Incarvito, A.D. Zuberbühler, A.L. Rheingold, K.D. Karlin, J. Am. Chem. Soc. 125 (2003) 634.
[37] D. Maiti, H.R. Lucas, A.A. NarducciSarjeant, K.D. Karlin, J. Am. Chem. Soc. 129 (2007) 6998.
[38] J. Shearer, C. Xin Zhang, L.N. Zakharov, A.L. Rheingold, K.D. Karlin, J. Am. Chem. Soc. 127 (2005) 5469.
[39] D. Petrovic, L.M.R. Hill, P.G. Jones, W.B. Tolman, M. Tamm, J. Chem. Soc., Dalton Trans. (2008) 887.
[40] M. Becker, F.W. Heinemann, F. Knoch, W. Donaubauer, G. Liehr, S. Schindler, G. Golub, H. Cohen, D. Meyerstein, Eur. J. Inorg. Chem. (2000) 719.
[41] D.A. Handley, P.B. Hitchcock, T.H. Lee, G.J. Leigh, Inorg. Chim. Acta 316 (2001) 59.
[42] T.P. Mitchell, W.H. Bernard, J.R. Wasson, Acta Crystallogr., B 26 (1970) 2096.
[43] L.M. Mirica, T.D.P. Stack, Inorg. Chem. 44 (2005) 2131.
[44] M.C. Kozlowski, X. Li, P.J. Carroll, Z. Xu, Organometallics 21 (2002) 4513.
[45] J. Mukherjee, R. Mukherjee, J. Chem. Soc., Dalton Trans. (2006) 1611.
[46] M. Toofan, A. Boushehri, Mazhar-UI-Haque, J. Chem. Soc., Dalton Trans. (1976) 217.
[47] I. Castro, J. Faus, M. Julve, C. Bois, J.A. Real, F. Lloret, J. Chem. Soc., Dalton Trans. (1992) 47.
[48] Y. Funahashi, K. Nakaya, S. Hirota, O. Yamauchi, Chem. Lett. 29 (2000) 1172.
[49] S. Herres, U. Flörke, G. Henkel, Acta Crystallogr., C 60 (2004) m659.
[50] D.L. Lewis, W.E. Hatfield, D.J. Hodgson, Inorg. Chem. 13 (1974) 147.
[51] M. Taki, S. Teramae, S. Nagatomo, Y. Tachi, T. Kitagawa, S. Itoh, S. Fukuzumi, J. Am. Chem. Soc. 124 (2002) 6367.
[52] V. Raab, K. Harms, J. Sundermeyer, B. Kovacevic, Z.B. Maksic, J. Org. Chem. 68 (2003) 8790.